Electrolytic production of nitrogen trifluoride from a molten CsF–HF–NH_4F system

Akimasa Tasaka, Kazuyoh Mizuno, Akira Kamata and Keiji Miki
Department of Applied Chemistry, Doshisha University, Imadegawa, Karasuma, Kamigyo-ku, Kyoto 602 (Japan)

Abstract

In order to decrease the vapor pressure of hydrogen fluoride (HF) and corrosion of the nickel anode in an electrolytic cell for the production of nitrogen trifluoride, the electrochemical behavior of nickel was investigated in the temperature range of 50–100 °C using a molten CsF–HF–NH_4F system

Anodic reaction on nickel seemed to vary with increasing potential, permitting division into four regions as follows anodic dissolution of nickel in Region I (0–1 V *vs* H_2), deposition of a Ni(II) compound on nickel in Region II (1–3 V), oxidation of Ni(II) film to Ni(III) and/or Ni(IV) compounds in Region III (3 5 V), and electrochemical fluorination of NH_3 in Region IV (more positive than 5 V) The addition of CsF to the molten electrolyte reduces the corrosion of the nickel anode and reduces the vapor pressure of HF in the melt A maximum current efficiency for NF_3 formation was recorded at 100 C.

Introduction

A large amount of gaseous fluorine compounds such as nitrogen trifluoride (NF_3), sulphur hexafluoride (SF_6), and tungsten hexafluoride (WF_6) are consumed by the electronics industry in Japan. Highly pure NF_3 (99.99%) free from carbon tetrafluoride (CF_4) is produced by electrolysis of molten NH_4F 2HF with a nickel anode to meet such demand

However, the high consumption of nickel anodes is troublesome. The corrosion of nickel anodes in NH_4F 2HF results in electrolytic current losses of more than 3% at 120 °C, resulting in deposition of nickel fluoride on the cell bottom and increased operating cost. The vapor pressure of HF in an NH_4F 2HF melt is as high as 297 mmHg at 120 °C [1], and HF is released with NH_3 from the cell. The gas pipe sometimes becomes plugged with an NH_4F deposit, resulting in explosions.

The objective of this work is to clarify the advantage of using a mixture of CsF, HF and NH_4F as the molten electrolyte for production of NF_3. The effect of the operating temperature on the current efficiency for NF_3 formation was also studied.

0022-1139/92/$5 00

Experimental

A small PTFE (polytetrafluoroethylene) cylinder-type cell of 0.45 dm^3 volume was provided for the electrochemical measurements and the corrosion test of nickel under operating conditions. The cell configuration has been described in detail in a previous paper [2]. A rod anode having an effective area of 0.07 cm^2 was located at the center of the cell, passing through the cell cover. A nickel sheet anode (purity 99.9%) having an effective area of 1 cm^2 was also used in certain cases. A large-area nickel counter cathode was used. Although the electrode potential was measured against the static potential of a platinum wire immersed in the same molten electrolyte, it was calibrated to a new scale referred to the potential for hydrogen evolution, and was presented in volts *vs.* H_2. The cell was positioned in a chamber filled with dry nitrogen to avoid moisture, and was warmed with a mantle heater to 50 or 80 °C.

Figure 1 illustrates the production cell. A Ni working anode of 50 cm^2 effective area located at the center of a cylinder-type copper cell (1.5 dm^3 volume) was separated by a copper skirt from the cell wall at which electrolytic hydrogen was evolved. The cell bottom was insulated by a PTFE sheet to avoid mixture of hydrogen with anode gas. The anode gas was treated with sodium fluoride (NaF) to eliminate HF. Its sample gas was fractionated by means of gas chromatography, and analyzed by

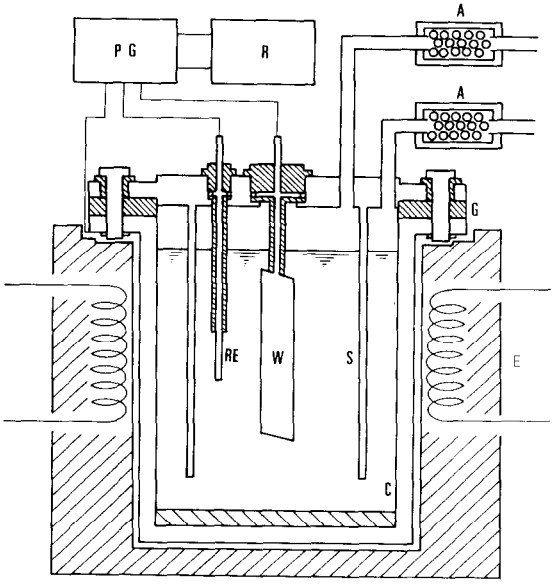

Fig. 1. Experimental setup for electrochemical fluorination. W: working electrode, Ni sheet; C: counter electrode, cell wall; RE: reference electrode, Pt wire; S: skirt; G: PTFE gasket; A: HF absorber, NaF pellets; PG: potentiostat - galvanostat; R: recorder; E: electric furnace.

infrared spectroscopy. The current efficiencies with respect to these constituents were evaluated from the results of gas analysis and the overall flow rate of anode gas.

Pre-electrolysis at low current density mainly with a carbon anode was conducted for many hours until NF_3 was generated and the electrolytic cell was stabilized before polarization measurement and/or corrosion testing. A Ni working electrode washed with water was rinsed with methanol to remove trace water prior to weighing. The anode was weighed before and after electrolysis to evaluate weight loss and the corresponding current losses. In this case, the concentration of water in the electrolyte could not be determined, but it might be less than 0.02 wt.% (about 21 mmol dm^{-3}) [3].

In experiments with the production cell, electrolyte was also prepared in a dry box with highly pure HF (99.99%), $NH_4F{\cdot}2HF$ (purity 99.7%) and cesium fluoride (purity better than 99%), but the cell was positioned in the atmosphere. Electrolysis was conducted soon after the electrolyte was charged in the cell. However, in our experiments it was not possible to determine the concentration of water in the melt.

Results and discussion

Anodic polarization measurements

Figure 2 shows the potential sweep curves of a nickel anode in $CsF{\cdot}NH_4F{\cdot}4HF$ at 50 °C. A large current caused by anodic dissolution of Ni flowed at the potential range of 0.3–0.5 V *vs.* H_2 when a fresh nickel

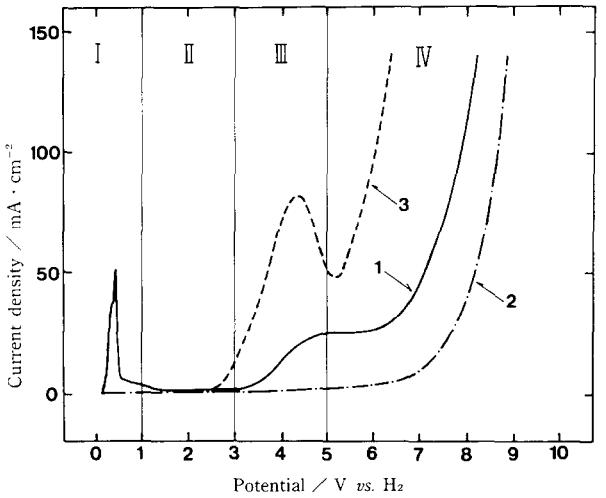

Fig. 2. Potential sweep curves of a nickel anode in molten $CsF{\cdot}NH_4F{\cdot}4HF$ at 50 °C; sweep rate = 200 mV s^{-1}; 1: first run, 2: second run, 3: 50th run.

anode was polarized (Curve 1), but it was subsequently passivated in the potential range of 1–3 V (Region II). The current increased again by oxidation and/or fluorination of the anode surface in the range of 3–5 V (Region III). At potentials higher than 6 V (Region IV), gas was evolved from the anode, and the current increased.

Curve 2 shows the polarization curve of the same specimen during the second run. No electrolytic current was observed over a wide range of potential until gas evolution took place at *ca.* 6 V, since the electrode surface was covered with a stable film. The surface film was not removed even if the electrode was left at the static potential for several minutes. Potential scanning in the range of 0–*ca.* 9 V was repeated many times. Curve 3 in Fig. 2 is the polarization curve after 50 runs. A large current was observed at potentials $> +3$ V. The current density moved up and down with the potential scan in the positive direction through a maximum of *ca.* 82 mA cm^{-2} at 4.3 V and a minimum of 50 mA cm^{-2} at 5 V, and increased thereafter. The polarization curve varied with the history of electrode.

Molten $CsF{\cdot}NH_4F{\cdot}4HF$ was electrolyzed with a fresh anode at given potentials, and the corrosion rate of the nickel anode was measured. The experimental results are summarized in Table 1. Note that the experiment was conducted under potentiostatic conditions, whereas polarization measurements such as shown in Fig. 2 were carried out by a potentiodynamic method. This causes different current densities under equal potential in the two cases (Fig. 2 and Table 1). Generally, the higher the sweep rate of potential, the higher the current density. As shown in Fig. 2, a large current caused by active dissolution of nickel was observed at 0.37 V. Table 1 shows that the electrolytic current was almost entirely consumed by the anodic dissolution. In the passive region, 1–3 V *vs.* H_2, the overall current density was small with no dissolution of Ni. The current density increased with increase of the anode potential above 5 V. Although the corrosion rate of the nickel anode also increased, the current losses were

TABLE 1

Weight losses of a nickel anode in molten $CsF{\cdot}NH_4F{\cdot}4HF$ at 50 °C against applied potential

Anode potential (V *vs.* H_2)	Overall current density (mA cm^{-2})	Corrosion rate (mg cm^{-2} h^{-1})	Current losses caused by Ni dissolution (%)
0.07	0.0114	0.00455	63.3
0.37	2.00	2.30	105
3.07	0.212	0.00	0
5.07	255	0.94	1.34
6.47	420	5.15	1.12
7.56	1180	16.8	1.30
9.47	3505	69.6	1.81

almost unchanged, at 1.1–1.8%. Electrolytic gas evolution took place at potentials $> +5$ V in Region IV of Fig. 2

It is difficult to identify the passive film or oxide layer on the anode surface, since the fluorine-containing nickel compound formed in the melt is decomposed when it is exposed to the atmosphere. However, its surface film is stable in the melt, and is built up by repetition of potential scanning, resulting in roughness.

With these experimental results and visual observations, we can evaluate the electrochemical processes occurring on the anode. After the virgin surface is dissolved in Region I, the anode is covered with a protective film, probably composed of a Ni(II) compound, either oxide or fluoride or both, in Region II. Nickel (II) film is oxidized to Ni(III) at potentials $> +3$ V. In the intermediate region, 3–5 V (Region III), NiO, which is a component of film, could form a spinel (Ni_3O_4) layer, which is electrochemically active and electrically conductive [4], and hence the electrolytic current of Curve 1 increases. Its layer is further oxidized to NiO_{2-x}, where x varies with the polarization potential; the higher the potential the smaller x. In the potential range $> +6$ V (Region IV), gas evolution takes place preferentially on the surface containing oxide. Once the oxide-containing film is formed during the first run of positive poten-

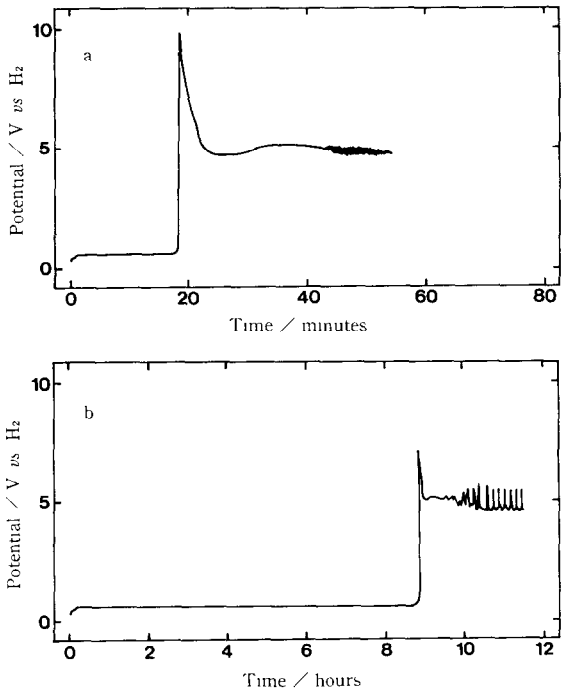

Fig 3 Chronopotentiograms of a nickel anode in molten CsF NH_4F 4HF at 50 C and given current densities (a) 25 mA cm $^{-2}$, (b) 10 mA cm $^{-2}$

tial scanning, the oxide in the layer is apparently not reduced even if the potential is scanned negatively, and hence no current flows in the potential range 0–6 V in the second run, with the exception of a very small current for passivation. The oxide-containing film thickens on repetitive potential scanning in the wide range of 0–9 V. Its brittle layer may crack and the nickel substrate may be exposed to the melt, resulting in a large current in Region III (Curve 3). Gas is evolved from a large surface at high rate (high current density) and relatively negative potential, *ca.* 5.5 V *vs.* H_2.

Figure 3 shows the chronopotentiograms of a fresh nickel electrode in molten $CsF{\cdot}NH_4F{\cdot}4HF$ at 50 °C. At 25 mA cm^{-2} (Curve a), the anode potential jumped to some 10 V *vs.* H_2 20 min after switch-on, then dropped to 5 V. This indicates that the formation of stable oxide-containing film requires 20 min or ~ 30 coulombs cm^{-2}. At 10 mA cm^{-2} (Curve b), on the other hand, the film containing oxide was formed only after 9 h. The potential fluctuated extensively after dropping to 5 V, probably because of degradation and regeneration of the layer composed of oxide and/or fluoride. In parallel with these processes, the fluorination of NH_3 to NF_3 takes place at 5 V *vs.* H_2. When electrolysis was conducted with the same nickel anode after pre-electrolysis at a potential lower than 3 V *vs.* H_2 for more than 10 h so as to eliminate residual water in the melt, the potential rose to higher than 10 V *vs.* H_2 even at low current density, and fluorination of NH_3 no longer took place. This indicates that the Ni anode was passivated, or covered with a stable oxide-containing film.

Effectiveness of CsF on the reduction of HF vapor pressure and corrosion of nickel anode

The corrosion test of the Ni anode was conducted under operating conditions of current density (25 mA cm^{-2}) and temperature (50 and 80 °C) for 22.2 h. The mole ratio of CsF to NH_4F was varied, while the ratio of HF to the sum of CsF and NH_4F was kept constant at 2. The current loss caused by Ni dissolution greatly decreased with increasing CsF concentration, as shown in Fig. 4.

The vapor pressure of HF over the NH_4F–HF melt at 50 and 80 °C was markedly lowered by a small addition of CsF, and was decreased even further when the CsF concentration became high.

High vapor pressures of HF and large corrosion rates of the nickel anode are major problems for the conventional process, as stated previously. These problems can be solved, or at least minimized, by the addition of CsF to the melt, although the reason and/or mechanism for this effect has not yet been clarified.

Electrolysis

Molten $CsF \cdot NH_4F{\cdot}4HF$ at 80 °C was electrolyzed at 20 mA cm^{-2} and the cell gas generated at the anode was collected and analyzed. While a large amount of O_2 was evolved for the first 25 h from decomposition of

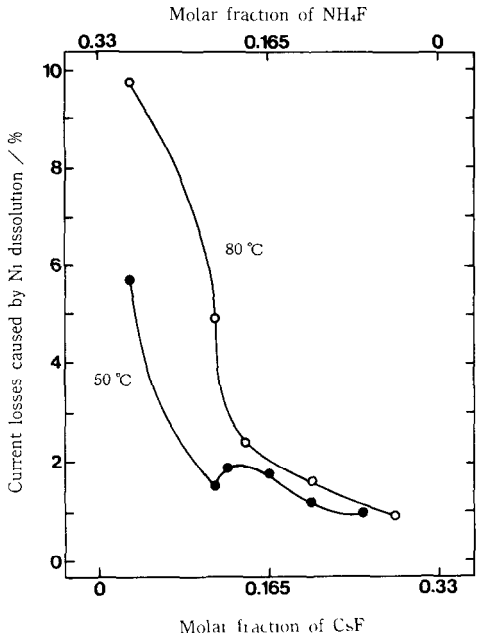

Fig 4 Effect of the CsF concentration on the anodic dissolution of nickel under galvanostatic electrolysis in molten $CsF-NH_4F-HF$ system at 25 mA cm^{-2} and 50 or 80 °C Amount of electricity in each experiment = 2000 C cm^{-2} (22 2 h)

residual water, the gas composition was stabilized thereafter, as illustrated in Fig. 5. It is clear that N_2 and NF_3 are the main products, with small amounts of O_2, N_2O, N_2F_2 and N_2F_4 being present.

Under the conditions of interest, NH_4^+ and NH_3 are in equilibrium, as shown in eqns (1) and (2):

$$NH_4F + nHF \rightleftharpoons NH_4^+ + F(HF)_n^- \quad (1)$$

$$NH_4^+ + mHF \rightleftharpoons NH_3 + H(HF)_m^+ \quad (2)$$

where $F(HF)_n^-$ and $H(HF)_m^+$ are the solvated ions of F^- and H^+, respectively, and now written as F^- and H^+ for simplicity. The amount of NH_3 in the melt is generally considered negligible. Nitrogen trifluoride and nitrogen are evolved at the anode by reactions (3)–(5) [5]:

$$NH_4^+ + 6F^- \longrightarrow NF_3 + 3HF + H^+ + 6e^- \quad (3)$$

$$2NH_4^+ + 6F^- \longrightarrow N_2 + 6HF + 2H^+ + 6e^- \quad (4)$$

$$2NH_4^+ \longrightarrow N_2 + 8H^+ + 6e^- \quad (5)$$

However, the side reactions (6)–(10) may also proceed in parallel to form

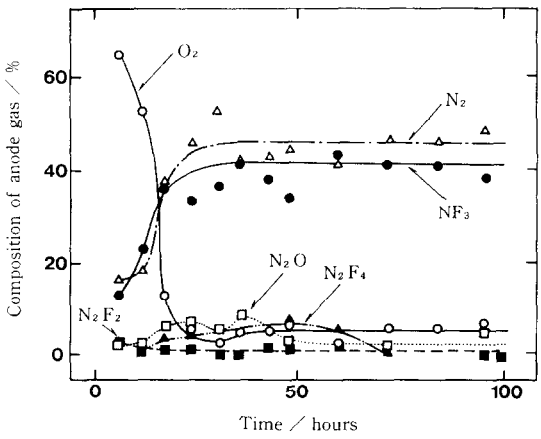

Fig. 5. Change in anode gas composition during galvanostatic electrolysis in molten $CsF{\cdot}NH_4F{\cdot}4HF$ at 20 mA cm^{-2} and 80 °C as a function of time. Conditions: nickel anode, surface area 50 cm^2, cell voltage 4.2 4.9 V, anode potential 3.7–4.3 V *vs.* Pt.

minor products, e.g. N_2F_2, N_2F_4, N_2O and O_2.

$$2NH_4^+ + 8F^- \longrightarrow N_2F_2 + 6HF + 2H^+ + 8e^- \quad (6)$$

$$2NH_4^+ + 10F^- \longrightarrow N_2F_4 + 6HF + 2H^+ + 10e^- \quad (7)$$

$$2NH_4^+ + H_2O + 8F^- \longrightarrow N_2O + 8HF + 2H^+ + 8e^- \quad (8)$$

$$2H_2O + 4F^- \longrightarrow O_2 + 4HF + 4e^- \quad (9)$$

$$2H_2O \longrightarrow O_2 + 4H^- + 4e^- \quad (10)$$

Since we have the percentage composition of these gases (Fig. 5) and the total volume produced, it is easy to calculate the current efficiency for NF_3 production and for all the gaseous products. The dotted line in Fig. 6 represents the current efficiency for NF_3 as a function of time, and the solid line the overall efficiency, showing that NF_3 is produced by electrolysis at a current efficiency of $\sim 37\%$.

Note that the overall efficiency for gaseous products is 93%. The current loss caused by Ni dissolution with an assumption of a two-electron transfer for the reaction:

$$Ni \longrightarrow Ni^{2+} + 2e^- \quad (11)$$

was estimated to be 4%. Thus, other current losses of some 3% also occurred. In galvanostatic electrolysis at 25 mA cm^{-2}, the current efficiency of gaseous products evolved at the anode was also about 90%.

Electrolysis of the $CsF{\cdot}NH_4F{\cdot}4HF$ melt was conducted with a nickel anode, and hydrogen was obtained from the cathode at a currrent efficiency of *ca.* 90%. However, the currrent efficiency for hydrogen evolution was increased by a further 5% when the nickel anode was substituted

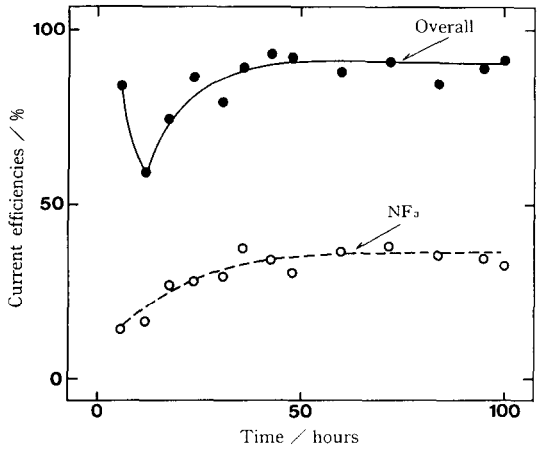

Fig. 6. Changes in current efficiencies for NF_3 formation and overall gas generated on a nickel anode during galvanostatic electrolysis in molten $CsF{\cdot}NH_4F{\cdot}4HF$ at 20 mA cm^{-2} and 80 °C as a function of time.

by an amorphous carbon anode. Consequently, we consider the oxidation/reduction sequence of nickel ions as a side reaction for the proposed process for making NF_3. Ni^{2+} in the vicinity of the anode is oxidized at the anode into Ni^{3+} and/or Ni^{4+}, depending on the anode potential:

$$Ni^{2+} \longrightarrow Ni^{3+} + e^- \quad (12)$$

$$Ni^{3+} \longrightarrow Ni^{4+} + e^- \quad (13)$$

$$Ni^{2+} \longrightarrow Ni^{4+} + 2e^- \quad (14)$$

These ions might migrate toward the cathode surface, and be reduced cathodically by the reverse reactions of (11) through (14) to consume current to some extent. These loss reactions are eliminated when the carbon anode is employed. It is clear that the disadvantage caused by corrosion of the nickel anode is great, and must be kept as low as possible. The addition of CsF into the melt helps achieve this purpose.

Although CsF seems to increase the rate of NF_3 formation by decreasing the anodic dissolution of nickel, further experiments must be conducted in order to prove it. The operating temperature is also an important process parameter. From experiments at 80, 100 and 120 °C, the maximum current efficiency for NF_3 formation was found to be 100 °C.

References

1 D. Filliaudeau and G. Picard, *Mater. Sci. Forum, 73–75* (1991) 669.
2 A. Tasaka, H. Itoh, T. Isogai, H. Aio and T. Tojo, *J. Electrochem. Soc., 138* (1991) 421.
3 T. Nakajima, T. Ogawa and N. Watanabe, *J. Electrochem. Soc., 134* (1987) 8.

4 J. A. Donohue, A. Zletz and R. J. Flannery, *J. Electrochem. Soc.*, *115* (1964) 1042; G. Wranglen, *An Introduction to Corrosion and Protection of Metals*, Kagaku Dojin, Kyoto, 1973, p. 125.
5 A. Tasaka, *Doctoral Thesis*, Kyoto University, 1970; N. Watanabe, A. Tasaka and K. Nakanishi, *Denki Kagaku*, *36* (1968) 685; *ibid.*, *37* (1969) 419, 481; A. Tasaka and N. Watanabe, *Z. Anorg. Allg. Chem.*, *385* (1971) 156.